Digestive and Liver Disease 51 (2019) 1050–1059

Contents lists available at ScienceDirect

Digestive and Liver Disease

journal homepage: www.elsevier.com/locate/dld

Oncology

Long noncoding RNA LINC00488 functions as a ceRNA to regulate hepatocellular carcinoma cell growth and angiogenesis through miR-330-5

Jun Gao [1], Xiangbao Yin [1], Xin Yu, Chao Dai, Fan Zhou *

Department of Hepatobiliary and Pancreatic Surgery, The Second Affiliated Hospital of Nanchang University, PR China

ARTICLE INFO

Article history:
Received 5 December 2018
Accepted 18 March 2019
Available online 17 April 2019

Keywords:
Angiogenesis
Apoptosis
LINC00488
Long non-coding RNA
microRNA-330-5p
Hepatocellular carcinoma
Proliferation
Talin-1

ABSTRACT

Background: Long non-coding RNAs (lncRNAs) recently have been identified as influential indicators in a variety of malignancies. Hence, the aim of the present study was to identify a functional lncRNA and its associated effects on hepatocellular carcinoma (HCC) in terms of cellular growth and a ngiogenesis.
Methods and results: Microarray-based analysis revealed a possible regulatory mechanism involving LINC00488, microRNA-330-5p (miR-330-5p) and talin-1 (TLN1) in HCC. Targetscan and RNA22 online tools predicted the relationship among LINC00488, miR-330-5p and TLN1, which were further validated by dual luciferase reporter gene assay, RNA pull-down and RIP. To evaluate the effects of LINC00488 and miR-330-5p on the cellular process of HCC, we performed a series of *in vitro* and *in vivo* experiments, with the expression of LINC00488, miR-330-5p, and TLN1 altered by delivering plasmids into Hep3B cell line. The obtained results demonstrated that cells with siRNA-mediated depletion of LINC00488 or restoration of miR-330-5p displayed suppressed abilities of *in vitro* proliferation as well as of *in vivo* tumor growth and angiogenesis, while *in vitro* apoptosis was notably induced.
Conclusion: The fundamental findings of the present study collectively propose that lncRNA LINC00488 can competitively sponge miR-330-5p to regulate TLN1 in relation to the cell growth and angiogenesis in HCC.

1. Introduction

Hepatocellular carcinoma (HCC) accounts for 70%–90% deaths related to primary liver cancer, which ranks the second leading cause of cancer-related deaths across the world, with a large number of patients diagnosed either at an intermediate or advanced stage [1,2]. It is well acknowledged that the global 5-year overall survival rate is still lower than 10%. Hence, if detected at an early stage, the patients with HCC have high chance to be cured successfully through operation, whose 5-year overall survival rate reaches more than 50% [3]. HCC patients diagnosed at an early-stage often benefit from potential therapeutic approaches including local ablative therapies, surgical resection or liver transplantation [4]. This being said, there is an urgent need for precise clinical diagnosis at the early stage of HCC, whereby molecular markers may prove to be useful tools regarding the appropriate understanding of molecular mechanisms underlying hepatocarcinogenesis [5]. In recent years, well-established evidence has revealed the function of non-coding genes especially long non-coding RNAs (lncRNAs), which display a distinct ability to regulate protein-coding and non-coding genes at transcriptional or post-transcriptional level, acting as a set of new regulators that participate in various cellular functions and disease processes [6]. Hence, this is intriguing and provides a fresh insight for investigation into the potential lncRNAs associated with HCC.

LncRNAs are RNA transcripts, longer than 200 nt, and are endowed with the ability to regulate transcription, translation, epigenetic modification, cell cycle and cellular differentiation [7]. For example, lncRNA fer-1-like family member 4 (FER1L4) has been reported to possess the ability to slow down the progression of HCC while the lncRNA DRHC has been implicated in the gradual process of HCC [8,9]. According to a recent study issued by Zhang et al., the cancer specific lncRNA profiles from The Cancer Genome Atlas (TCGA) found that the expression of LNC00488 is up-regulated in HCC [10]. Besides, the interaction between microRNAs (miRNAs) and lncRNAs within cells has been shown to be one representative regulation pattern of miRNAs and should be discussed due to

* Corresponding author at: Department of Hepatobiliary and Pancreatic Surgery, The Second Affiliated Hospital of Nanchang University, No. 1, Mingde Road, Nanchang 330006, Jiangxi Province, PR China.
E-mail address: zhoufan_zf@126.com (F. Zhou).
[1] These authors contributed equally to this work.

https://doi.org/10.1016/j.dld.2019.03.012
1590-8658/

their large number [11]. In particular, highly up-regulated lncRNA HULC in liver cancer has been indicated to serve as an endogenous "sponge" to down-regulate miRNAs activities [12]. A previous study demonstrated that the overexpression of miR-330 is related to poor prognosis and results in more aggressive phenotypes of HCC [13]. Studies have shown that miR-330-5p is regulated by tumor oncogenic lncRNA MIAT in epithelial ovarian cancer, by lncRNA HOTAIR in atherosclerosis and by lncRNA DGCR5 in non-small cell lung cancer [14–16]. Through microarray-based analysis, we subsequently proposed a hypothesis of a mechanical regulatory relationship between LINC00488 and miR-330-5p. Furthermore, the involvement of TLN1, a gene encoding a cytoplasmic protein Talin-1, has been documented to exert inhibitory effects in prostate cancer as a bid to miR-124 [17], highlighting its possible mutual effect in connection with miRNAs. In addition, TLN1 functions as a promising diagnostic marker for HCC with its higher specificity and sensitivity [18]. Hence, the central objective of the study was to decipher the roles of LINC00488 and miR-330-5p associated with TLN1 in HCC and thereby provide a deep understanding of the lncRNA function in HCC.

2. Materials and methods

2.1. Ethics statement

The current study was performed with the approval of the Institutional Review Board of The Second Affiliated Hospital of Nanchang University. Written informed consent was obtained from each participant. All animal experiments were performed in strict accordance with the recommendations in the Guide for the Care and Use of Laboratory Animals of the National Institutes of Health. The protocol of animal experiments was approved by the Institutional Animal Care and Use Committee of The Second Affiliated Hospital of Nanchang University.

2.2. Microarray-based analysis

The expression of TLN1 in HCC of TCGA database was analyzed using starBase (http://starbase.sysu.edu.cn/panGeneDiffExp.php). The prediction regarding the possible upstream regulatory miRNA for TLN1 was performed in connection with the following 6 databases, TargetScan (http://www.targetscan.org/vert_71/), starBase (http://starbase.sysu.edu.cn/agoClipRNA.php?source=mRNA), mirDIP (http://ophid.utoronto.ca/mirDIP/index.jsp#r), miRDB (http://mirdb.org/miRDB/index.html), DIANA (http://diana.imis.athena-innovation.gr/DianaTools/index.php?r=microT_CDS/index) and miRSearch (https://www.exiqon.com/miRSearch), from which the intersection of which was obtained. The upstream regulatory lncRNA for miR-330-5p was predicted with the use of the RNA22 database (https://cm.jefferson.edu/rna22/Precomputed/) and Redundant Arrays of Independent Drives (RAID) database (http://www.rna-society.org/raid/search.html).

2.3. Study subjects and cell culture

A total of 46 cases of HCC comprised of 32 males and 14 females, were selected from The Second Affiliated Hospital of Nanchang University between April 2016 to April 2017. There were 19 patients aged ≤50 years and 27 aged >50 years; 28 with a tumor size <5 cm and 18 with tumor size ≥5 cm. The paracancerous tissues 5 cm from the carcinomas were collected and regarded as the controls. The tumors were categorized according to tumor-nodes-metastasis (TNM) classification as follows: stage I, n = 18; stage II, n = 13; stage III, n = 15. Partial fresh tissues were preserved in liquid nitrogen at −80 °C for reverse transcription quantitative polymerase chain reaction (RT-qPCR) purposes with the intention of determining the expression of LINC00488 and miR-330-5p while the remaining were fixed in 10% neutral formalin, embedded with paraffin and sectioned for immunohistochemistry (IHC) and TLN1 quantification.

Human normal liver cell line L02 (derived from human fetal liver) and human HCC cell lines (Huh-7, Hep3B, HCCLM3 and MHCC97) purchased from Shanghai Xiangfu Biotechnology Co., Ltd., (Shanghai, China) were subjected to gene expression examinations. Cells were cultured in Roswell Park Memorial Institute (RPMI) 1640 complete medium supplemented with 10% fetal bovine serum (FBS), 100 U/mL penicillin and 100 μg/mL streptomycin in an incubator at 37 °C with 5% CO_2 and saturated humidity. Half of the medium was changed after a 48-h culture period and changed once every 3 days. When cell confluence had reached 80%–90%, the cells were detached with 0.25% trypsin and constructed into a single-cell suspension. The expression of LINC00488 and miR-330-5p in human normal liver cell line L02 and human HCC cell lines (Huh-7, Hep3B, HCCLM3 and MHCC97) was examined through the application of RT-qPCR, with the cell line exhibiting the highest LINC00488 expression employed for subsequent experiments.

2.4. Immunohistochemistry (IHC)

The tissue specimen was fixed in 10% neutral formalin (DF0113, Beijing Solarbio Life Sciences Co., Ltd., Beijing, China), embedded with paraffin and sectioned at a thickness of 4 μm. The slices were baked at 60 °C for 1 h and conventionally dewaxed by xylene (YB-5485, Shanghai Yu Bo Biological Technology Co., Ltd., Shanghai, China), followed by hydration with gradient alcohol. Next, 3% H_2O_2 was employed to immerse the slices at room temperature for 20 min in order to eliminate endogenous peroxidase activity. Antigen recovery methods were conducted twice, after which blockade with 10% goat serum for 15 min was performed. The slices were then incubated first with primary rabbit antibody to TLN1 (1:1000, ab71333, Abcam Inc., Cambridge, MA, UK) at 4 °C overnight, followed by secondary biotin-labeled goat anti-rabbit antibody to immunoglobulin G (IgG) (1:1000, ab6721, Abcam Inc., Cambridge, MA, UK) at 37 °C for 40 min. Afterwards, the slices were visualized by diaminobezidin (DAB) (DA1010, Beijing Solarbio Life Sciences Co., Ltd., Beijing, China) and stained with hematoxylin (H8070, Beijing Solarbio Life Sciences Co., Ltd., Beijing, China). Phosphate buffer saline (PBS) was employed as the negative control (NC) replacing the primary antibody. The results were examined and scored by two independent observers using the double-blinded method. Five fields of high power were selected in a random fashion under the guidance of an optical microscope (CX41-12C02, Olympus Corp., Tokyo, Japan). Cells with brown yellow-colored particles inside were regarded as positive cells.

2.5. Cell treatments

Human HCC cell line displaying the highest LINC00488 expression was selected for subsequent experiments. Following trypsinization of the selected sub-cultured cells at passage 3, the cells were seeded into 24-well plates. The culture liquid was removed until the cells were observed to have grown into a monolayer. The cells were then intervened with si-NC, si-LINC00488, mimic-NC, miR-330-5p mimic, inhibitor-NC, miR-330-5p inhibitor, si-NC, si-TLN1 and miR-330-5p mimic + pcDNA TLN1 plasmids, respectively. The cells were seeded 24 h prior to transfection until cell confluence reached 50%–60%. Cell transfection was conducted in accordance with the instructions of the lipofectamine 2000 (11668–019, Invitrogen Inc., Carlsbad, CA, USA).

2.6. *RNA fluorescence* in situ *hybridization (RNA-FISH)*

The sub-cellular localization of LINC00488 in HCC cells was obtained using bioinformatics tools available at http://lncatlas.crg.eu/ and identified by means of FISH following the instructions of Ribo™ lncRNA FISH Probe Mix (Red) (Ribobio Co., Ltd., Guangzhou, Guangdong, China). The coverslip was placed in a 24-well plate, where cells were seeded at a density of 6×10^4 cells/well. When cell confluence reached approximately 80%, the plate was fixed with 1 mL of 4% paraformaldehyde, and treated with proteinase K (2 μg/mL), glycine and acetylation reagent. The cells were prehybridized with 250 μL prehybridization solution at 42 °C for 1 h and then hybridized with 250 μL hybridization solution containing LINC00488 probe (300 ng/mL) at 42 °C overnight. The nucleus was stained with phosphate-buffered saline with Tween-20 (PBST)-diluted 4′,6-diamidino-2-phenylindole (DAPI) (1 : 800) in the 24-well plate for 5 min. The coverslips where the cells had migrated to were then mounted with a quenching agent for fluorescence detection. Five fields were randomly selected for microscopic observation and photography under a fluorescence microscope (Olympus Corp., Tokyo, Japan).

2.7. *Dual-luciferase reporter gene assay*

Bioinformatics prediction website (https://cm.jefferson.edu/rna22/Interactive/) was used to ascertain as to whether binding sites existed between LINC00488 and miR-330-5p as well as between miR-330-5p and the 3′-untranslated region (3′-UTR) of TLN1. Next, pmirGLO Dual-Luciferase miRNA Target Expression Vector (Promega Corp., Madison, WI, USA) was performed to construct wild type-LINC00488 (Wt-LINC00488) and mutant type-LINC00488 (Mut-LINC00488) vectors. The binding site between LINC00488 and miR-330-5p was determined by means of dual-luciferase reporter gene assay. A full length of LINC00488 gene was inserted between the two enzyme sites, Xho I and Xba I. The PCR products were detached by Xho I and Xba I and sub-cloned into the psiCHECK-2 vector. The cells were seeded into a 6-well plate with 2×10^5 cells/well and transfected in accordance with the aforementioned method. The successfully transfected cells were collected after a 48-h culture period. The effects of miR-330-5p on luciferase activity of 3′-UTR of TLN1 were detected based on the instructions provided by the dual-luciferase detection kit (D0010, Beijing Solarbio Life Sciences Co., Ltd., Beijing, China). Glomax20/20 luminometer (E5311, Shaanxi Zhongmei Biotechnology Co., Ltd., Xi'an, Shaanxi, China) was utilized for fluorescence intensity determination. The experiment was repeated 3 times.

2.8. *RNA-pull down and RNA immunoprecipitation (RIP)*

The Hep3B cells were manipulated with 50 nM biotin-labeled Wt-bio-LINC00488 RNA and Mut-bio-LINC00488 RNA for 48 h. The cells were collected, and then incubated in the specific lysate buffer (Ambion, Austin, Texas, USA) for 10 min. The lysates were incubated with the M-280 streptavidin beads (S3762, Sigma-Aldrich Chemical Company, St. Louis, MO, USA) that were pre-coated with RNase-free bovine serum albumin (BSA) and yeast tRNA (TRNABAK-RO, Sigma-Aldrich Chemical Company, St. Louis, MO, USA). Following incubation at 4 °C for 3 h, the beads were washed twice with pre-cooled lysate buffer solution, low-salt buffer solution 3 times and high-salt buffer solution on one occasion. The combined RNAs were purified by Trizol, while miR-330-5p enrichment was examined by RT-qPCR.

Next, the binding of LINC00488 RNA to argonaute-2 (AGO2) protein was detected using a RIP kit (Millipore, Temecula, CA, USA). Following pre-cooled PBS washing, the supernatant was discarded. The cells were lysed using a radioimmunoprecipitation assay (RIPA) lysis of equal volume (P0013B, Beyotime Biotechnology Co., Ltd., Beijing, China) in an ice bath for 5 min, followed by collection of the supernatant *via* centrifugation (14,000 rpm, 10 min, 4 °C). A section of the cell extract was used as the input while the remaining part was incubated with antibody to AGO2 (ab32381, 1:50, Abcam Inc., Cambridge, MA, UK) at room temperature for 30 min for co-precipitation while IgG (ab109489, 1:100, Abcam Inc., Cambridge, MA, UK) which served as a NC.

Table 1
Primer sequences for RT-qPCR.

Gene	Primer sequences (5′ – 3′)
LINC00488	F: CAATACTGACCACATCCACGTC R: GGGTCTGGCTCACTGTCTTTA
miR-330-5p	F: CCCAGGAGGACTGAAGCAACAA R: GCTATCTCAGGGCTTGTTGCTTC
TLN1	F: TGTGCCAATGGCTACCTGGA R: GAACCAGCCACACGCTTTGA
Caspase-3	F: AACTGGACTGTGGCATTGAG R: ACAAAGCGACTGGATGAACC
CyclinD1	F: CTGTGCGCCCTCCGTATCTTA R: GGCGGCCAGGTTCCACTTGAG
Bax	F: TGCCAGCAAACTGGTGCTCA R: GCACTCCCGCCACAAAGATG
Bcl-2	F: CGCATCAGGAAGGCTAGAGT R: AGCTTCCAGACATTCGGAGA
GAPDH	F: GAAGGTCGGAGTCAACGGATTT R: ATGGGTGGAATCATATTGGAAC
U6	F: GTGCCTGCTTCGGCAGCACATA R: TGGAACGCTTCACGAATTTGCGTGTC

Notes: RT-qPCR, reverse transcription quantitative polymerase chain reaction; LINC, long intergenic noncoding; miR, microRNA; TLN1, Talin-1; Bcl-2, B-cell lymphoma 2; Bax, Bcl-2-associated X protein; GAPDH, glyceraldehyde 3-phosphate dehydrogenase; F, forward; R, reverse.

2.9. *RNA isolation and quantification*

Total RNA was extracted from the sample using an ultrapure RNA extraction kit (D203-01, Beijing GenStar Co., Ltd., Beijing, China). The primer sequences of LINC00488, miR-330-5p, TLN1, Caspase-3, CyclinD1, B-cell lymphoma 2 (Bcl-2), Bcl-2-associated X protein (Bax), glyceraldehyde 3-phosphate dehydrogenase (GAPDH) and U6 were designed and then synthesized by TaKaRa Biotechnology Co., Ltd. (Dalian, Liaoning, China) as listed in Table 1. The reaction was performed in connection with instructions of TaqMan MicroRNA Assays Reverse Transcription Primer (4366596, Thermo Scientific Pierce, Waltham, MA, USA). All the samples were processed on ABI PRISM® 7300 (Prism®7300, Shanghai Kunke Instrument Co., Ltd., Shanghai, China) according to the manual of SYBR® Premix Ex TaqTM II kit (RR820A, Action-Award Biotechnology Co., Ltd., Guangzhou, Guangdong, China). U6 was employed as the endogenous control for miR-330-5p and GAPDH for LINC00488, TLN1, Caspase-3, CyclinD1, Bax and Bcl-2. The fold changes were calculated by means of relative quantification ($2^{-\Delta\Delta Ct}$ method). The experiment was repeated 3 times.

2.10. *Western blot analysis*

Total protein was extracted using a RIPA kit (R0010, Beijing Solarbio Life Sciences Co., Ltd., Beijing, China). The cells were lysed by protein lysis (60% RIPA + 39% sodium dodecyl sulfate (SDS) +1% protease inhibitor) on ice for 30 min and then centrifuged (13,500 rpm, 30 min, 4 °C). The protein concentration of the supernatant was determined using a bicinchoninic acid (BCA) kit (Shanghai Jining Shiye Co., Ltd., Shanghai, China). After that, the cell lysates were separated by SDS-polyacrylamide gel electrophoresis (SDS-PAGE) (300 V, 30 min) and transferred onto a nitrocellulose membrane by means of wet transfer. Membrane blockade was

conducted using 5% BSA for 1 h at room temperature and incubated with diluted primary antibodies (Abcam Inc., Cambridge, MA, UK): rabbit antibodies to TLN1 (ab71333, 1:1000), Cleaved Caspase-3 (ab32042, 1:500), CyclinD1 (ab134175, 1:10000), Bax (ab32503, 1:400) and Bcl-2 (ab59348, 1:500) overnight 4 °C. The membranes were then incubated with the horseradish peroxidase (HRP)-conjugated goat anti-rabbit secondary antibody to IgG (1:5000, Beijing Zhongshan Biotechnology Co., Ltd., Beijing, China). The results were visualized with an exposure machine, with GAPDH regarded as an internal control. The film was scanned, the gray value was measured using the Wes automatic protein blot quantification analysis system, after which the relative ratio was calculated and subsequently compared with the internal reference. The experiment was repeated 3 times in each group.

2.11. Flow cytometry

After 48 h of transfection, propidium (PI) (40710ES03, Shanghai Qcbio Co., Ltd., Shanghai, China) single staining method was performed in order to investigate the cell cycle distribution of Hep3B cells in connection with the detection of red fluorescence at an excitation wavelength of 488 nm using a flow cytometer (FACSCalibur, BD, FL, NJ, USA). Hep3B cells were detached with 0.25% trypsin. The supernatant was aspirated by means of centrifugation (4 °C, 1000 r/min, 5 min), followed by an additional around of centrifugation (1000 r/min, 5 min). After the supernatant had been removed, the cells were fixed with pre-cooled 70% ethanol at 4 °C overnight, and subsequently centrifuged (1000 r/min, 5 min). Following incubation with 10 μL of RNase at 37 °C for 5 min, 1% PI staining was performed under condition void of light for 30 min at room temperature. The experiment was repeated 3 times.

After 48-h transfection and detachment by ethylenediaminetetraacetic acid (EDTA)-free trypsin, Hep3B cells were collected and centrifuged (4 °C, 1000 r/min, 5 min) with the supernatant discarded. The cells were subjected to centrifugation (1000 r/min, 5 min). Following the removal of the supernatant, Hep3B cell apoptosis was detected using an Annexin V-fluorescein isothiocyanate (FITC)/PI apoptosis detection kit (CA1020, Beijing Solarbio Life Sciences Co., Ltd., Beijing, China) using a flow cytometer. After binding buffer washing, the cells were re-suspended in a mixture of Annexin-V-FITC and binding buffer (1:40), followed by incubation at room temperature for 30 min. The incubation was permitted to continue for an additional 15 min at room temperature followed by the addition of the mixture of Annexin-V-FITC and Binding buffer (1:40). The experiment was repeated 3 times.

2.12. 5-Ethynyl-2′-deoxyuridine (EdU) assay

When cell confluence reached approximately 80%, Cell-Light^{TM} EdU fluorescence microscope detection kit (C10301, Ribobio Co., Ltd., Guangzhou, Guangdong, China) was employed for Hep3B cell proliferation detection in accordance with the manufacturer's instructions. The Hep3B cells were exposed to 50 μM EdU (100 μL/well) for 2 h, fixed with PBS containing 4% paraformaldehyde (100 μL/well) at room temperature for 15–30 min and incubated with 2 mg/mL glycine for 10 min. The cells were permeabilized with PBS comprised of 0.5% TritonX-100 (100 μL/well) and stained with 100 μL 1X Apollo dye liquor at room temperature for 30 min under conditions void of light. Incubation was continued following the addition of 100 μL Hoechst33342 at room temperature for 10–30 min in dark. After treating with Hoechst33342, microscopic observation was performed under the guidance of a fluorescence microscope. At least 3 fields were then selected from each well.

2.13. Xenograft tumor in nude mice

A total of 30 nude mice were housed in a laminar flow room of specific pathogen free (SPF)-level at constant temperature in a constant humid environment where padding, drinking water and feed were autoclaved. Hep3B cells were cultured, collected and made into cell suspension (1×10^6 cells/100 μL) by PBS. Cell suspension (0.2 mL) was inoculated subcutaneously using a syringe (1 mL) on the back of the nude mice. Each cell line was inoculated into 6 nude mice, all of which were then housed in a SPF animal room. Tumor formation was observed on a weekly basis with the tumor size recorded and the data obtained used to create a growth curve. The tumor size was based on the following formula: tumor size = 1/2 (long diameter × short diameter^2). Five weeks later, all nude mice were euthanized, followed by the collection of tumors with the tumor weight recorded and tumor volume calculated.

The intratumor microvascular density (MVD) was assessed as a biomarker for angiogenesis. IHC staining of CD34 (monoclonal antibody, Zymed Laboratories, San Diego, Southern California, USA) was performed in accordance with the method prescribed by Weidner et al. [19] as a reference of CD34 positive. Any brown-colored vascular endothelial cell or endothelial cell cluster, which was clearly separated from adjacent microvessels, tumor cells, and other connective tissue elements, was considered as a single microvessel and a MVD value. Areas exhibiting the highest neovascularization were detected by means of scanning the tumor sections at a low power. After the area with the highest neovascularization was identified, individual microvessel counts were made on a 400 × field. The cells that were vague or blurred were excluded. Five fields were randomly selected with the mean value obtained.

2.14. Statistical analysis

All experimental data were analyzed using the Statistic Package for Social Science (SPSS) 19.0 statistical software (IBM Corp., Armonk, NY, USA). The experiments were repeated 3 times. Measurement data were expressed as mean ± standard deviation. Comparisons between two groups were analyzed by *t*-test. Comparisons among multiple groups were analyzed by one-way analysis of variance (ANOVA), and tumor volumes at different time points were compared by repeated measurement ANOVA, followed by Tukey's post hoc test. A $p < 0.05$ was considered to be statistically significant.

3. Results

3.1. TLN1 is highly expressed in HCC and regulated by miR-330-5p

According to literature review, TLN1 plays important roles in multiple tumors [20,21], yet the role of TLN1 in HCC remains unclear. As per the TCGA database, data obtained indicating that TLN1 was highly expressed in HCC (Fig. 1A). In order to further understand the regulatory mechanism of TLN1, 6 different databases including TargetScan were utilized to predict the potential miRNA that could regulate the expression of TLN1 in relation to the intersection results (Fig. 1B), which revealed there to be 2 miRNAs (miR-330-5p and miR-326) in the intersection. The score for the binding of has-miR-330-5p to TLN1 was much higher than that of miR-326 to TLN1. Mounting evidence has indicated the regulatory function of miR-330-5p in different tumors as a competing endogenous RNA (ceRNA) [16,22,23]. Therefore, miR-330-5p was then identified as the subject for further investigation. Meanwhile, in order to elucidate the mechanism by which miR-330-5p and TLN1 influence HCC, RNA22 and RAID databases were employed to

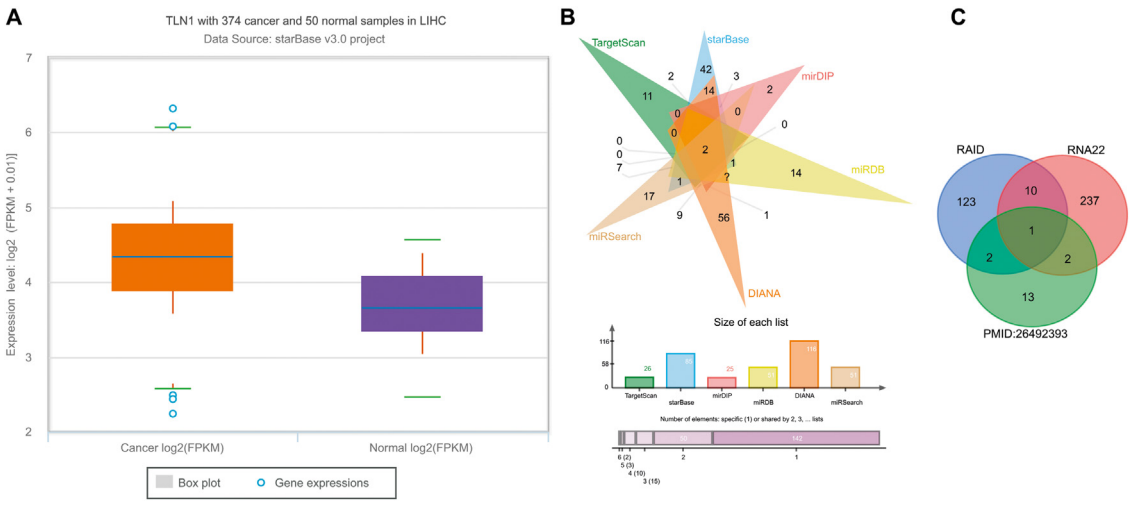

Fig. 1. Microarray-based analysis identifies highly expressed TLN1 in HCC and the potential regulatory mechanism. (A) relative expression of TLN1 in HCC according to TCGA; the abscissa indicates the sample type and the ordinate indicates the gene expression; the box plot on the left represents TLN1 expression in HCC samples and the box plot on the right represents TLN1 expression in normal samples; (B) prediction on miRNA that can regulate TLN1 expression; triangles in 6 different colors represent predication results obtained from 6 different databases with the intersection in the middle; (C) prediction regarding a lncRNA that can regulate miR-330-5p expression; circles in 3 different colors represent predication results obtained from RAID database, RNA22 database and the reported study [21] with the intersection showing in the middle; TLN1, talin-1; HCC, hepatocellular carcinoma; TCGA, The Cancer Genome Atlas; miRNA/miR, microRNA; lncRNA, long non-coding RNA; RAID, redundant Arrays of Independent Drives.

make predictions regarding the possible lncRNA that could regulate the miR-330-5p expression. Recently, a published study indicated that 18 lncRNAs were highly expressed in HCC [10]. However, there was only one lncRNA, namely LINC00488, detected within the intersection of RNA22 database, RAID database as well as the above-mentioned published study, which was also found to be highly expressed in HCC. These findings suggest that, LINC00488 can affect the progression of HCC and act to potentially regulate the expression of miR-330-5p, which targets TLN1 and regulates its expression.

3.2. *LINC00488 is highly expressed in HCC tissues and cell lines*

The first step in our experiment was to verify the expression of LINC00488 in paracancerous and HCC tissues through RT-qPCR, the results of which revealed that LINC00488 was notably expressed at a higher level in HCC tissues than in the paracancerous tissues ($p < 0.05$, Fig. 2A). Besides, the expression of LINC00488 in HCC stage I, II and III was shown in Fig. 2B, suggesting that compared with HCC stage I, LINC00488 was highly expressed in HCC stage II and III ($p < 0.05$). Furthermore, the selection process was performed based in relation to the expression of LINC00488 in human normal liver cell line L02 and HCC cell lines (Huh-7, Hep3B, HCCLM3 and MHCC97). Compared with L02 cell line, the LINC00488 expression in the HCC cell lines was markedly increased (all $p < 0.05$, Fig. 2C), among which the Hep3B cell line exhibited the highest LINC00488 expression. Therefore, the HCC cell line Hep3B was selected for the subsequent experiments.

3.3. *Silencing of LINC00488 inhibits Hep3B cell proliferation and angiogenesis while inducing cell apoptosis*

With the results in the above section detailing the altered expression of LINC00488 in HCC, the following experiments were designed to observe the cellular function of LINC00488. FISH was conducted in order to determine the subcellular localization of LINC00488, the results of which revealed that LINC00488 (green) was predominantly distributed in the cytoplasm (Fig. 3A) with blue representing the nucleus. Subsequently, in order to evaluate the regulation of LINC00488 on factors related to cell proliferation and apoptosis, RT-qPCR and western blot analysis were applied for the quantification of the expression of LINC00488, CyclinD1, Bcl-2, Cleaved Caspase-3 and Bax in Hep3B cells with the varying expression of LINC00488, both of which were also assessed by EdU assay and flow cytometry. Compared with the cells manipulated with si-NC, the cells manipulated with si-LINC00488 exhibited a lower expression of LINC00488 and TLN1, a lower cell proliferation rate, in addition to increased miR-330-5p expression, higher apoptosis rate, more cells arrested at the G0/G1 stage and fewer cells at S stage (all $p < 0.05$, Fig. 3B–F) while the protein expression of CyclinD1 and Bcl-2 were down-regulated and those of cleaved Caspase-3 and Bax were up-regulated (all $p < 0.05$, Fig. 3F). Next, the xenograft tumor in nude mice was conducted in order to measure MVD value, which is widely considered to be a morphological measure of tumor angiogenesis. The results demonstrated that si-LINC00488 considerably diminished the intratumor MVD and tumor volume (both $p < 0.05$, Fig. 3G–H). Based on the aforementioned results, we arrived at the conclusion that silencing LINC00488 can inhibit Hep3B cell proliferation and tumor angiogenesis and promote cell apoptosis.

3.4. *LINC00488 competitively sponges miR-330-5p and miR-330-5p negatively regulates TLN1*

Following the elucidation on the role of LINC00488 in HCC, the next step was to identify the potential molecular mechanism. Based on the prediction results provided by the bioinformatics website, specific binding sites between miR-330-5p and LINC00488 were identified. Dual-luciferase reporter gene assay was employed to further ascertain as to whether LINC00488 could competitively sponge miR-330-5p since relative luciferase activity of LINC00488-Wt was obviously weakened by miR-330-5p mimic while no similar reduction was observed in relation to the luciferase activity of LINC00488-Mut 3′UTR when compared to the mimic NC treatment ($p < 0.05$, Fig. 4A).

RNA-pull down and RIP assays were conducted in order to further verify the interaction between LINC00488 and miR-330-5p. The results of RNA pull-down assay indicated that when compared with LINC00488-Mut, relative miR-330-5p enrichment was significantly increased in LINC00488-Wt ($p < 0.05$, Fig. 4B), suggesting that miR-330-5p and LINC00488 could directly bind to each other.

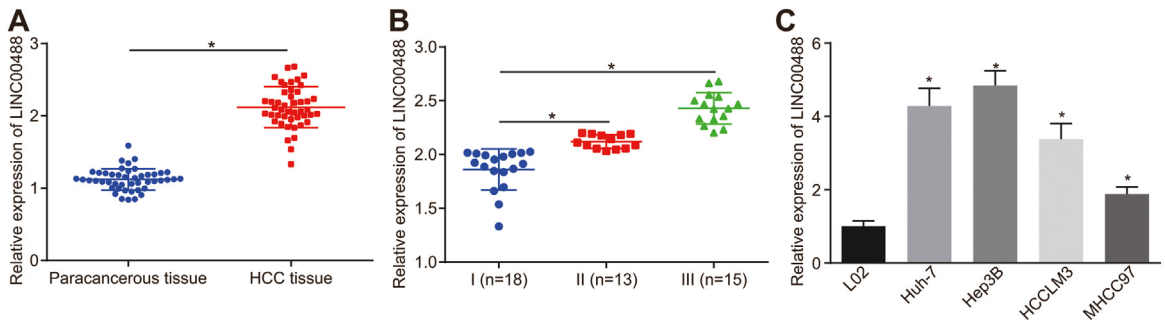

Fig. 2. LINC00488 is highly expressed in HCC tissues and cells. (A) relative expression of LINC00488 in paracancerous tissues (n = 46) and HCC tissues (n = 46) determined by RT-qPCR, *$p < 0.05$ *vs.* the paracancerous tissues; (B) relative expression of LINC00488 in HCC stage I (n = 18), II (n = 13) and III (n = 15) detected by RT-qPCR, *$p < 0.05$ *vs.* the HCC patients at stage I; (C) relative expression of LINC00488 in human normal liver cell line L02 and HCC cell lines (Huh-7, Hep3B, HCCLM3 and MHCC97) determined by RT-qPCR, *$p < 0.05$ *vs.* the L02 cell line; the data are measurement data and expressed as mean ± standard deviation; comparison was analyzed by *t*-test between two groups and by one-way analysis of variance among multiple groups, followed by the Tukey's post hoc test; the experiment was repeated 3 times; LINC, long intergenic noncoding; HCC, hepatocellular carcinoma; RT-qPCR, reverse transcription quantitative polymerase chain reaction.

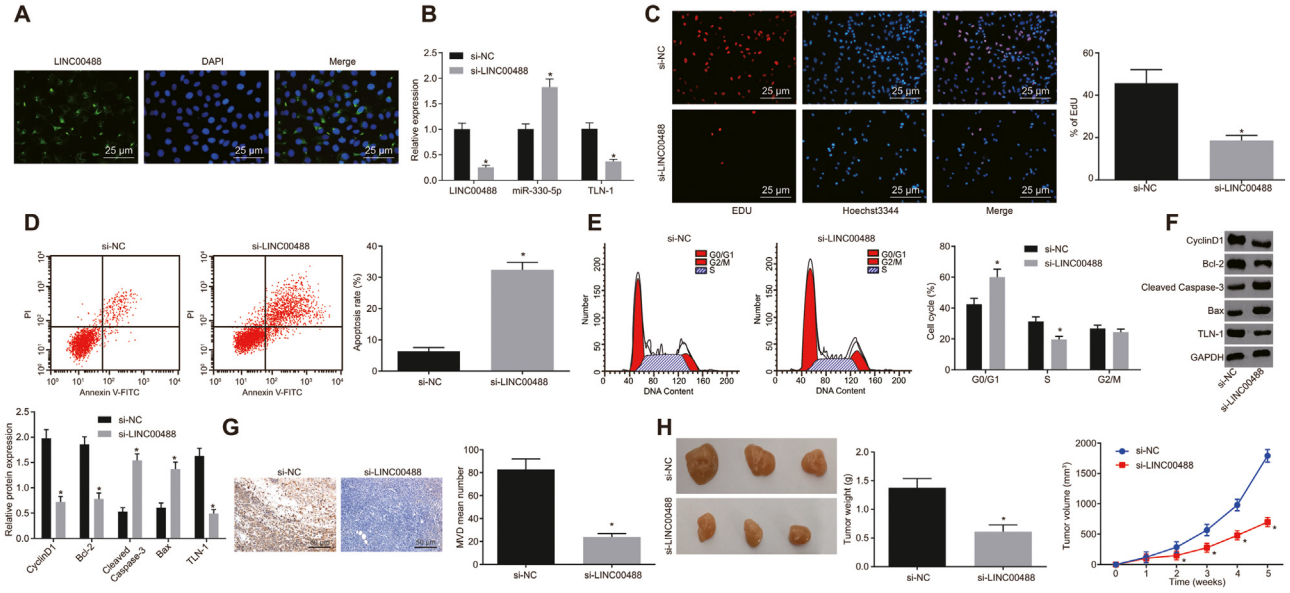

Fig. 3. Silencing LINC00488 exerts inhibitory effects on Hep3B cell proliferation and angiogenesis and promoting effects on cell apoptosis. (A) subcellular localization of LINC00488 detected by FISH (× 400); (B) relative expression of LINC00488, miR-330-5p and TLN1 in cells treated with si-NC and si-LINC00488 determined by RT-qPCR; (C) cell proliferation in cells treated with si-NC and si-LINC00488 detected by EdU assay (×200); (D) cell apoptosis in cells treated with si-NC and si-LINC00488 detected by flow cytometry; (E) cell cycle distribution in cells treated with si-NC and si-LINC00488 detected by flow cytometry; (F) relative protein expression of cell proliferation-related factor (CyclinD1) and cell apoptosis-related factors (Bcl-2, Cleaved Caspase-3 and Bax) determined by western blot analysis; (G) MVD value measured by means of tumor xenograft procedure in nude mice (×200); (H) tumor weight and volume resected from nude mice treated with si-NC and si-LINC00488; *$p < 0.05$ *vs.* the cells or mice treated with si-NC; the data are measurement data and expressed as mean ± standard deviation; comparison was analyzed by *t*-test between two groups; the experiment was repeated 3 times; LINC, long intergenic noncoding; FISH, fluorescence *in situ* hybridization; RT-qPCR, reverse transcription quantitative polymerase chain reaction; EdU, 5-Ethynyl-2′-deoxyuridine; Bcl-2, B-cell lymphoma-2; Bax, Bcl-2 associated protein X; MVD, microvascular density; NC, negative control. (For interpretation of the references to colour in the text, the reader is referred to the web version of this article.)

The RIP assay applied demonstrated that when compared with IgG, the relative LINC00883 enrichment in AGO2 was notably elevated ($p < 0.05$, Fig. 4C), highlighting that LINC00883 could bind to AGO2 protein. Based on the aforementioned results, it was concluded that LINC00883 can competitively sponge miR-330-5p.

In order to deepen our understanding of the relationship between miR-330-5p and TLN1, the bioinformatics website was explored for predictive results. The predictive results obtained revealed that there were specific binding sites on 3′-UTR of TLN1 for miR-330-5p. Further evidence was collected by a dual-luciferase reporter gene assay which demonstrated that miR-330-5p mimic was able to suppress the relative luciferase activity of TLN1-Wt compared with mimic-NC ($p < 0.05$,) while no significance regarding relative luciferase activity of TLN1-Mut was detected ($p > 0.05$, Fig. 4D), indicating that miR-330-5p could target TLN1.

RT-qPCR was then employed for investigation on the possible regulatory role of miR-330-5p on TLN1 (Fig. 4E). The results revealed that miR-330-5p expression increased and TLN1 expression decreased in cells manipulated with miR-330-5p mimic in contrast to mimic-NC treatment ($p < 0.05$). Compared with si-NC intervention, miR-330-5p expression did not differ significantly in cells treated with siRNA against TLN1, which lowered the TLN1 expression ($p < 0.05$). Besides, miR-330-5p expression exhibited a remarkable increase following treatment of miR-330-5p mimic + pcDNA TLN1 or miR-330-5p mimic only ($p < 0.05$) in comparison to cells without any intervention. The above data provided verification, suggesting that TLN1 is a target gene of miR-330-5p and regulated negatively by miR-330-5p.

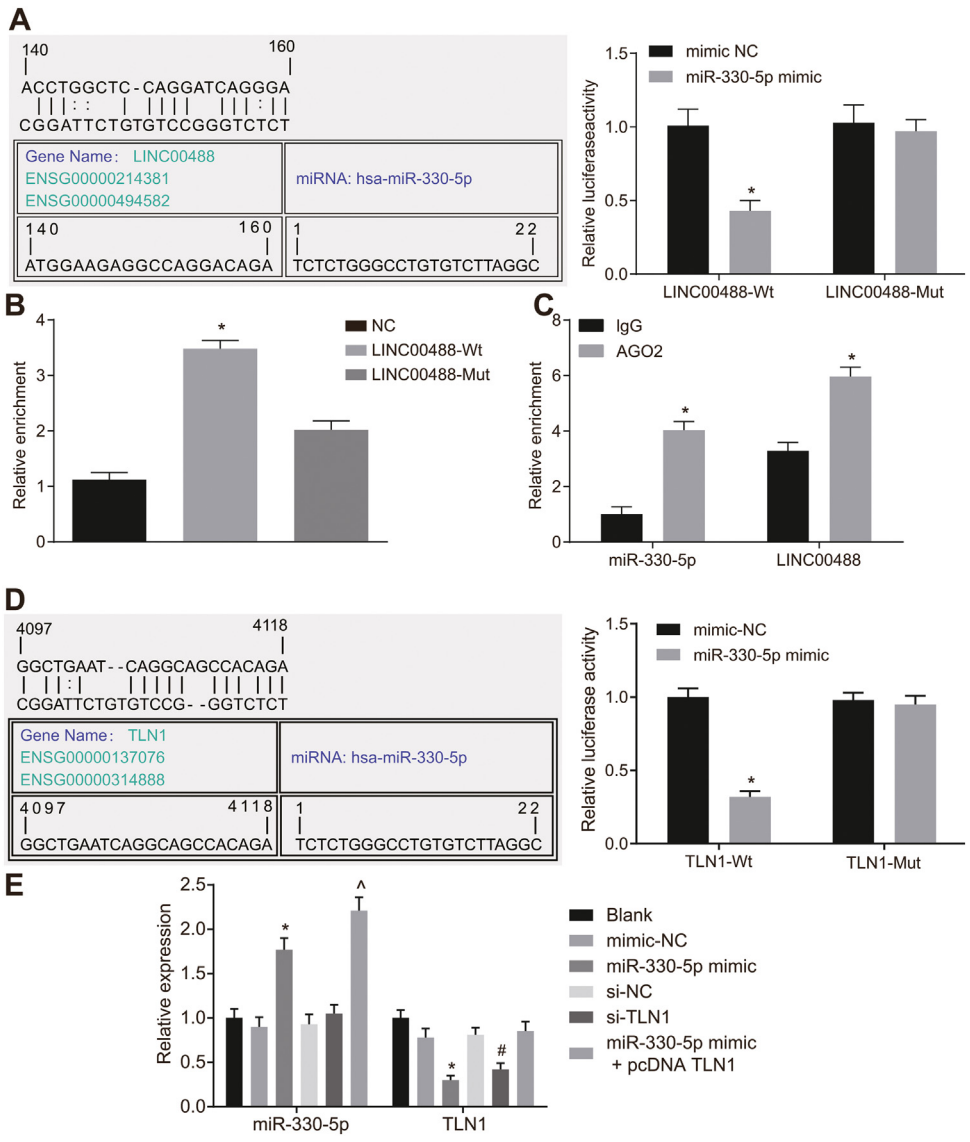

Fig. 4. LINC00488 competitively binds to miR-330-5p and miR-330-5p targets TNL1. (A) binding sites between LINC00488 and miR-330-5p, and relative luciferase activity determination in cells treated with the reporter plasmids and either miR-330-5p mimic or mimic NC, $^{*}p < 0.05$ *vs.* the cells treated with mimic NC; (B) relative enrichment of miR-330-5p to LINC00488-Wt and LINC00488-Mut analyzed by RNA pull-down assay, $^{*}p < 0.05$ *vs.* the LINC00488-Mut; (C) relative enrichment of AGO2 to miR-330-5p and LINC00488 detected by RIP assay, $^{*}p < 0.05$ *vs.* the enrichment of IgG; (D) binding sites between TLN1 and miR-330-5p, and relative luciferase activity determination in cells treated with the reporter plasmids and either miR-330-5p mimic or mimic NC, $^{*}p < 0.05$ *vs.* the cells treated with mimic NC; (E) relative expression of miR-330-5p and TLN1 in cells with the presence of different expression of miR-330-5p and TLN1 determined by RT-qPCR, $^{*}p < 0.05$ *vs.* the cells treated with mimic NC, $\#p < 0.05$ *vs.* the cells treated with si-NC, $\hat{}p < 0.05$ *vs.* the cells treated with miR-330-5p mimic; the data are measurement data and expressed as mean ± standard deviation; comparison was analyzed by *t*-test between two groups and by one-way analysis of variance among multiple groups, followed by the Tukey's post hoc test; the experiment was repeated 3 times; LINC, long intergenic noncoding; miR, microRNA; NC, negative control; Wt, wild type; Mut, mutant; AGO2, Argonaute 2; RIP, RNA immunoprecipitation; miR, microRNA; TLN1, Talin-1; RT-qPCR, reverse transcription quantitative polymerase chain reaction.

3.5. Resorted miR-330-5p negatively mediating TLN1 inhibits tumorigenesis of HCC

After the demonstration of the anti-tumor effects of LINC00488, the focus of the experiment was then shifted to the regulatory mechanism of miR-330-5p in HCC cell functions in association with TLN1. RT-qPCR was conducted to investigate the altered expression of miR-330-5p and TLN1 in HCC, the results of which indicated that miR-330-5p was expressed at a lower level while that of TLN1 was expressed at a markedly higher level among the HCC tissues in comparison to the paracancerous tissue ($p < 0.05$, Fig. 5 A). In order to determine the positive expression rate of TLN1, IHC was performed, the results of which revealed that positive expression rate of TLN1 was much higher in HCC tissues than that in paracancerous tissues ($p < 0.05$, Fig. 5B). For verification purposes, RT-qPCR was employed to determine the relative expression of miR-330-5p in human normal liver cell line L02 and HCC cell lines (Huh-7, Hep3B, HCCLM3 and MHCC97). The results confirmed that 4 HCC cell lines all exhibited lower miR-330-5p expression and higher TLN1 expression than human normal liver cell line L02 (all $p < 0.05$, Fig. 5C). Combined with the results of RT-qPCR and IHC, we concluded that miR-330-5p is poorly expressed in HCC tissue while TLN1 is opposite.

Following transfection, HCC cell biological behaviors *in vitro* affected by miR-330-5p or TLN1 were analyzed by means of western blot analysis, EdU assay and flow cytometry. The results illustrated that when miR-330-5p increased, relative protein expression of CyclinD1 and Bcl-2 was down-regulated, and Cleaved Caspase-3 and Bax was up-regulated, which indicated that cell proliferation was blocked and cell apoptosis was accelerated in comparison to mimic-NC intervention ($p < 0.05$). Similar results

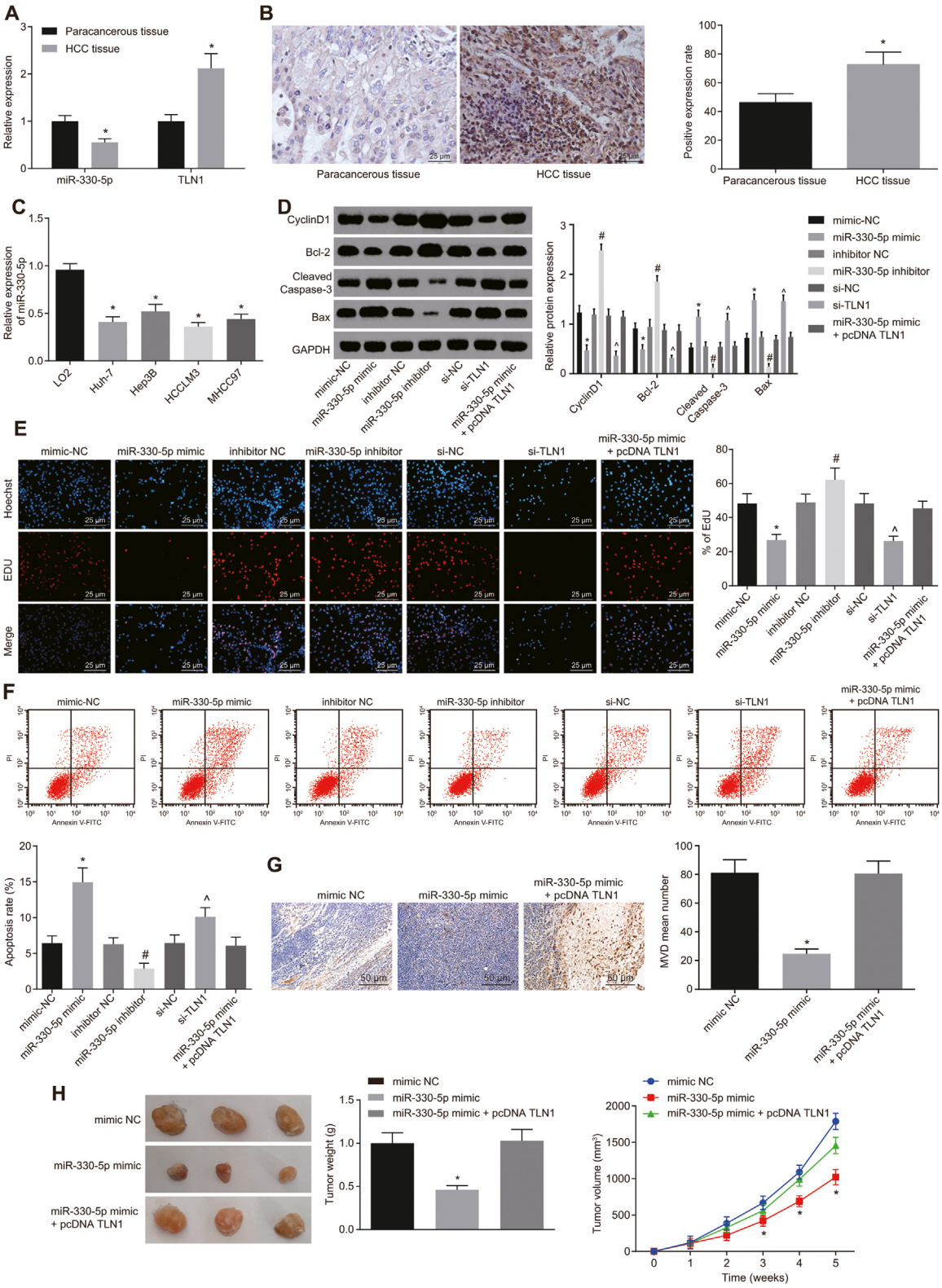

Fig. 5. Elevated miR-330-5p weakens the proliferation ability of Hep3B cells and *in vivo* tumor angiogenesis while strengthening Hep3B cell apoptosis by negatively mediating TLN1. (A) relative expression of miR-330-5p and TLN1 in paracancerous tissues and HCC tissues determined by RT-qPCR, *$p < 0.05$ *vs.* the paracancerous tissues; (B) positive expression of TLN1 in paracancerous tissues and HCC tissues detected by immunohistochemistry (×200), *$p < 0.05$ *vs.* the paracancerous tissues; (C) relative expression of miR-330-5p and TLN1 in human normal liver cell line L02 and HCC cell lines (Huh-7, Hep3B, HCCLM3 and MHCC97) determined by RT-qPCR, *$p < 0.05$ *vs.* the L02 cell line; (D) relative protein expression of cell proliferation-related factor (CyclinD1) and cell apoptosis-related factors (Bcl-2, Cleaved Caspase-3 and Bax) determined by western blot analysis; (E) cell proliferation in cells treated with different expression patterns of miR-330-5p and TLN1 detected by EdU assay (×200); (F) cell apoptosis in cells treated with different expression patterns of miR-330-5p and TLN1 detected by flow cytometry; *$p < 0.05$ *vs.* the cells treated with mimic NC, #$p < 0.05$ *vs.* the cells treated with inhibitor NC, ^$p < 0.05$ *vs.* the cells treated with si-NC; (G) MVD value measured by means of tumor xenograft in nude mice (×200); (H) tumor weight and volume resected from nude mice with the presence of elevated miR-330-5p; *$p < 0.05$ *vs.* the mice treated with mimic NC; the data are measurement data and expressed as mean ± standard

were observed among cells manipulated with siRNA against TLN1 in comparison to the si-NC intervention ($p < 0.05$). A contradictory trend was observed in cells introduced with miR-330-5p inhibitor in contrast to inhibitor NC intervention ($p < 0.05$). However, no significant differences were found in the cells treated with miR-330-5p mimic + pcDNA TLN1 compared with mimic-NC intervention, si-NC intervention or inhibitor NC intervention ($p > 0.05$, Fig. 5D–F).

Intratumor MVD was regarded as a marker of tumor angiogenesis *in vivo* through xenograft tumor in nude mice. Key observations were made indicating that miR-330-5p mimic was capable of reducing the value of MVD while diminishing tumor volume was detected when compared with mimic-NC treatment ($p < 0.05$) with no significant differences detected following miR-330-5p mimic + pcDNA TLN1 treatment ($p > 0.05$, Fig. 5G–H). Consequently, these findings suggest that Hep3B cell proliferation is inhibited and cell apoptosis is induced *in vitro* while tumor angiogenesis is suppressed *in vivo* in the event of miR-330-5p elevation.

4. Discussion

As the third leading cause of cancer related deaths worldwide, HCC has a notably high rate of recurrence of approximately 70% hepatic resection within 5 years, which is a commonly applied for certain patients especially suffering from early HCC [24,25]. Therefore, efforts should be made to comprehensively understand early development of HCC. A previous meta-analysis revealed that a group of lncRNAs that either highly or poorly expressed in HCC may offer potential prognostic indicators for therapeutic intervention [26]. In the current study, attempts were made to elucidate the roles of LINC00488 and miR-330-5p in hepatocarcinogenesis. The results obtained provided verification regarding our initial hypothesis that Hep3B cell proliferation *in vitro* and tumor angiogenesis *in vivo* are inhibited while Hep3B cell apoptosis *in vitro* is elevated with the presence of LINC00488 silencing or the restoration of miR-330-5p as well as the down-regulated TLN1.

A key finding of the current study revealed there to be high expression of TLN1 along with poor miR-330-5p expression in the HCC samples. Evidence was collected indicating that TLN1 was targeted and negatively regulated by miR-330-5p. TLN1 has been identified as an oncogene exhibiting high levels of expression in HCC cells contributing to various processes in HCC progression, including cell growth, tumor metastasis and ion transport [27]. TLN1 knockdown exerts inhibitory effects on HCC MHCC-97L cell migration in the malignant processes of HCC [28]. Therefore, the up-regulation of TLN1 in HCC was indicated to potentially play a functional role in relation to tumor progression, highlighting a role as a prognostic marker [29]. Apart from miR-330-5p, certain miRNAs such as miR-9, have been shown to share a negative correlation with the expression of TLN1, miR-9 may participate in metastasis and adhesion of HCC by regulating TLN1 [30], which was consistent with the findings of the current study whereby miR-330-5p was found to target and negatively regulate TLN1.

In the present study, it was observed that elevated miR-330-5p could act to down-regulate the expression of TLN1 and further weaken the proliferative and angiogenic abilities of Hep3B cells, which ultimately slows down the progression of HCC. Angiogenesis is understood to be a process characterized by new vessels formation from previous blood vessels, leading to lumen formation and finally nascent vessel stabilization [31]. Due to the fact that an oncogenic event may offer tumor cells access to strengthened survival ability beyond surveillance, blood supply is required during the dynamic tumor growth, shedding light on the critical role of tumor angiogenesis [32]. A recent study concluded that angiogenesis is the master regulator in hepatocarcinogenesis [33]. Accumulating evidence has suggested the function of non-coding RNA is tightly linked to angiogenesis. For instance, the significance of miRNAs in angiogenesis has also been reported. miR-451 has been found as a suppressor of tumor angiogenesis in regard to highly vascularized HCC tumors [34]. The inhibitory effects of miR-29b on tumor angiogenesis in breast cancer have also demonstrated by targeting Akt3 protein [35]. Regarding lncRNA, on the other hand, evidence has revealed the crucial roles of lncRNAs in angiogenesis induction *via* both direct and indirect means to regulate tumor growth [36]. MVD has been shown to be a reliable marker capable of evaluating angiogenic status when introduced to cancer tissues [37]. Elevated MVD in HCC may reflect lower survival rate and higher risk of recurrence [38]. Consistently, observations were made in this study where nude mice with silenced LINC00488 had smaller tumors and lower MVD value, highlighting the anti-angiogenic effects exerted by LINC00488 inhibition.

Mechanically speaking, the results of the study revealed a relationship between LINC00488 and miR-330-5p indicating that LINC00488 could competitively sponge miR-330-5p. Similar lncRNA-miRNA mechanism in HCC has been reported that the knockdown of the lncRNA HOXA cluster antisense RNA2 (HOXA-AS2), which is also highly expressed in HCC, suppresses HCC cell proliferation and promotes cell apoptosis *via* the miR-520c-3p/glypican-3 axis [39]. Likewise, lncRNA metastasis-associated lung adenocarcinoma transcript 1 (MALAT1) has been shown to sponge miR-30a-5p, and silenced MALAT1 and restored miR-30a-5p could suppress HCC cell migration and invasion [40]. In addition, lncRNA CRNDE has also been indicated to be capable of facilitating HCC cell proliferation, migration and invasion *via* the miR-217/mitogen-activated protein kinase 1 axis [41]. Therefore, regulation mode of lncRNA-miRNA is universal molecular interaction in tumor progression.

To sum up, this present study suggests that silencing of LINC00488 and restored miR-330-5p can facilitate the treatment of patients with HCC by inhibiting HCC cell proliferation *in vitro* and angiogenesis *in vivo*. In addition, our study indicated that LINC00488 competitively sponged miR-330-5p to up-regulate levels of TLN1, CyclinD1 and Bcl-2 and down-regulate levels of Cleaved Caspase-3 and Bax, which alters cell cycle distribution, promotes cell proliferation and inhibits apoptosis (Supplementary Fig. 1). However, the present study did not investigate the detailed regulatory molecules of LINC00488 expression in liver. Yet, this issue will sure be well-solved when the study of lncRNA is more thorough in the near future.

Conflict of interest

None declared.

Acknowledgment

This study was supported by Key Foundation of Jiangxi Provincial Science and Technology Department (No. 20171ACB21064),

deviation; comparison was analyzed by *t*-test between two groups and by one-way analysis of variance among multiple groups; tumor volumes at different time points are analyzed by repeated measurement analysis of variance, followed by the Tukey's post hoc test; the experiment was repeated 3 times; miR, microRNA; TLN1, Talin-1; HCC, hepatocellular carcinoma; RT-qPCR, reverse transcription quantitative polymerase chain reaction; Bcl-2, B-cell lymphoma-2; Bax, Bcl-2 associated protein X; EdU, 5-Ethynyl-2′-deoxyuridine; MVD, microvascular density; NC, negative control.

Youth Science Foundation of Jiangxi Provincial Science and Technology Department (No. 20151BAB205105), Jiangxi Provincial Science and Technology Planning Project (No. 20141BBG70042), and Science Planning Project of Jiangxi Provincial Education Department (No. GJJ14049).

Appendix A. Supplementary data

Supplementary material related to this article can be found, in the online version, at doi:https://doi.org/10.1016/j.dld.2019.03.012.

References

[1] Vilgrain V, Pereira H, Assenat E, et al. Efficacy and safety of selective internal radiotherapy with yttrium-90 resin microspheres compared with sorafenib in locally advanced and inoperable hepatocellular carcinoma (SARAH): an open-label randomised controlled phase 3 trial. Lancet Oncol 2017;18:1624–36.
[2] Fink A, Hassan MA, Okan NA, et al. Early interactions of murine macrophages with Francisella tularensis map to mouse chromosome 19. MBio 2016;7:e02243.
[3] Lin XJ, Chong Y, Guo ZW, et al. A serum microRNA classifier for early detection of hepatocellular carcinoma: a multicentre, retrospective, longitudinal biomarker identification study with a nested case-control study. Lancet Oncol 2015;16:804–15.
[4] Granito A, Bolondi L. Non-transplant therapies for patients with hepatocellular carcinoma and Child-Pugh-Turcotte class B cirrhosis. Lancet Oncol 2017;18:e101–12.
[5] Cao C, Sun J, Zhang D, et al. The long intergenic noncoding RNA UFC1, a target of MicroRNA 34a, interacts with the mRNA stabilizing protein HuR to increase levels of beta-catenin in HCC cells. Gastroenterology 2015;148, 415-26 e18.
[6] Huang J, Zhou N, Watabe K, et al. Long non-coding RNA UCA1 promotes breast tumor growth by suppression of p27 (Kip1). Cell Death Dis 2014;5:e1008.
[7] De Clara E, Gourvest M, Ma H, et al. Long non-coding RNA expression profile in cytogenetically normal acute myeloid leukemia identifies a distinct signature and a new biomarker in NPM1-mutated patients. Haematologica 2017;102:1718–26.
[8] Wang X, Dong K, Jin Q, et al. Upregulation of lncRNA FER1L4 suppresses the proliferation and migration of the hepatocellular carcinoma via regulating PI3K/AKT signal pathway. J Cell Biochem 2018, http://dx.doi.org/10.1002/jcb.27980.
[9] Zhuang R, Zhang X, Lu D, et al. lncRNA DRHC inhibits proliferation and invasion in hepatocellular carcinoma via c-Myb-regulated MEK/ERK signaling. Mol Carcinog 2018, http://dx.doi.org/10.1002/mc.22934.
[10] Zhang J, Fan D, Jian Z, et al. Cancer specific long noncoding RNAs show differential expression patterns and competing endogenous RNA potential in hepatocellular carcinoma. PLoS One 2015;10:e0141042.
[11] Yang G, Lu X, Yuan L. LncRNA: a link between RNA and cancer. Biochim Biophys Acta 2014;1839:1097–109.
[12] Wang J, Liu X, Wu H, et al. CREB up-regulates long non-coding RNA, HULC expression through interaction with microRNA-372 in liver cancer. Nucleic Acids Res 2010;38:5366–83.
[13] Hu X, Feng Y, Sun L, et al. Roles of microRNA-330 and its target gene ING4 in the development of aggressive phenotype in hepatocellular carcinoma cells. Dig Dis Sci 2017;62:715–22.
[14] Shao S, Tian J, Zhang H, et al. LncRNA myocardial infarction-associated transcript promotes cell proliferation and inhibits cell apoptosis by targeting miR-330-5p in epithelial ovarian cancer cells. Arch Med Sci 2018;14:1263–70.
[15] Liu J, Huang GQ, Ke ZP. Silence of long intergenic noncoding RNA HOTAIR ameliorates oxidative stress and inflammation response in ox-LDL-treated human macrophages by upregulating miR-330-5p. J Cell Physiol 2018, http://dx.doi.org/10.1002/jcp.27317.
[16] Wang R, Dong HX, Zeng J, et al. LncRNA DGCR5 contributes to CSC-like properties via modulating miR-330-5p/CD44 in NSCLC. J Cell Physiol 2018;233:7447–56.
[17] Zhang W, Mao YQ, Wang H, et al. MiR-124 suppresses cell motility and adhesion by targeting talin 1 in prostate cancer cells. Cancer Cell Int 2015;15:49.
[18] Youns MM, Abdel Wahab AH, Hassan ZA, et al. Serum talin-1 is a potential novel biomarker for diagnosis of hepatocellular carcinoma in Egyptian patients. Asian Pac J Cancer Prev 2013;14:3819–23.
[19] Weidner N. Intratumor microvessel density as a prognostic factor in cancer. Am J Pathol 1995;147:9–19.
[20] Luo D, Zhan S, Xia W, et al. Proteomics study of serum exosomes from papillary thyroid cancer patients. Endocr Relat Cancer 2018;25:879–91.
[21] Manso AM, Okada H, Sakamoto FM, et al. Loss of mouse cardiomyocyte talin-1 and talin-2 leads to beta-1 integrin reduction, costameric instability, and dilated cardiomyopathy. Proc Natl Acad Sci U S A 2017;114:E6250–9.
[22] Hang D, Zhou J, Qin N, et al. A novel plasma circular RNA circFARSA is a potential biomarker for non-small cell lung cancer. Cancer Med 2018;7:2783–91.
[23] Fu X, Zhang L, Dan L, et al. LncRNA EWSAT1 promotes ovarian cancer progression through targeting miR-330-5p expression. Am J Transl Res 2017;9, 4094-103.
[24] Kumar DP, Santhekadur PK, Seneshaw M, et al. A novel regulatory role of apoptosis antagonizing transcription factor in the pathogenesis of NAFLD and HCC. Hepatology 2018, http://dx.doi.org/10.1002/hep.30346.
[25] Marasco G, Colecchia A, Colli A, et al. Role of liver and spleen stiffness in predicting the recurrence of hepatocellular carcinoma after resection. J Hepatol 2018, http://dx.doi.org/10.1016/j.jhep.2018.10.022.
[26] Chen S, Zhang Y, Wu X, et al. Diagnostic value of lncRNAs as biomarker in hepatocellular carcinoma: an updated meta-analysis. Can J Gastroenterol Hepatol 2018;2018:8410195.
[27] Chen P, Zheng X, Zhou Y, et al. Talin-1 interaction network promotes hepatocellular carcinoma progression. Oncotarget 2017;8:13003–14.
[28] Fang KP, Dai W, Ren YH, et al. Both Talin-1 and Talin-2 correlate with malignancy potential of the human hepatocellular carcinoma MHCC-97 L cell. BMC Cancer 2016;16:45.
[29] Kanamori H, Kawakami T, Effendi K, et al. Identification by differential tissue proteome analysis of talin-1 as a novel molecular marker of progression of hepatocellular carcinoma. Oncology 2011;80:406–15.
[30] Sun J, Fang K, Shen H, et al. MicroRNA-9 is a ponderable index for the prognosis of human hepatocellular carcinoma. Int J Clin Exp Med 2015;8:17748–56.
[31] Thabut D, Shah V. Intrahepatic angiogenesis and sinusoidal remodeling in chronic liver disease: new targets for the treatment of portal hypertension? J Hepatol 2010;53:976–80.
[32] Lu Z, Zhang W, Gao S, et al. MiR-506 suppresses liver cancer angiogenesis through targeting sphingosine kinase 1 (SPHK1) mRNA. Biochem Biophys Res Commun 2015;468:8–13.
[33] Raoul JL, Gilabert M, Adhoute X, et al. An in-depth review of chemical angiogenesis inhibitors for treating hepatocellular carcinoma. Expert Opin Pharmacother 2017;18:1467–76.
[34] Liu X, Zhang A, Xiang J, et al. miR-451 acts as a suppressor of angiogenesis in hepatocellular carcinoma by targeting the IL-6R-STAT3 pathway. Oncol Rep 2016;36:1385–92.
[35] Li Y, Cai B, Shen L, et al. MiRNA-29b suppresses tumor growth through simultaneously inhibiting angiogenesis and tumorigenesis by targeting Akt3. Cancer Lett 2017;397:111–9.
[36] Kumar MM, Goyal R. LncRNA as a therapeutic target for angiogenesis. Curr Top Med Chem 2017;17:1750–7.
[37] Miyata Y, Sakai H. Reconsideration of the clinical and histopathological significance of angiogenesis in prostate cancer: usefulness and limitations of microvessel density measurement. Int J Urol 2015;22:806–15.
[38] Li Y, Ma X, Zhang J, et al. Prognostic value of microvessel density in hepatocellular carcinoma patients: a meta-analysis. Int J Biol Markers 2014;29:e279–87.
[39] Zhang Y, Xu J, Zhang S, et al. HOXA-AS2 promotes proliferation and induces epithelial-mesenchymal transition via the miR-520c-3p/GPC3 Axis in hepatocellular carcinoma. Cell Physiol Biochem 2018;50:2124–38.
[40] Pan Y, Tong S, Cui R, et al. Long non-coding MALAT1 functions as a competing endogenous RNA to regulate vimentin expression by sponging miR-30a-5p in hepatocellular carcinoma. Cell Physiol Biochem 2018;50:108–20.
[41] Wang H, Ke J, Guo Q, et al. Long non-coding RNA CRNDE promotes the proliferation, migration and invasion of hepatocellular carcinoma cells through miR-217/MAPK1 axis. J Cell Mol Med 2018;22:5862–76.